

Sensitivity of spin structures of small spin-1 condensates against a magnetic field studied beyond the mean field theory

C.G. Bao[‡]

Center of Theoretical Nuclear Physics, National Laboratory of Heavy Ion Accelerator, Lanzhou, 730000, People's Republic of China

State Key Laboratory of Optoelectronic Materials and Technologies, School of Physics and Engineering, Sun Yat-Sen University, Guangzhou, 510275, People's Republic of China

E-mail: stsbcg@mail.sysu.edu.cn

Abstract. The spin structures of small spin-1 condensates ($N \leq 1000$) under a magnetic field B has been studied beyond the mean field theory (MFT). Instead of the spinors, the many body spin-eigenstates have been obtained. We have defined and calculated the spin correlative probabilities to extract information from these eigenstates. The correlation coefficients and the fidelity susceptibility have also been calculated. Thereby the details of the spin-structures responding to the variation of B can be better understood. In particular, from the correlation coefficients which is the ratio of the 2-body probability to the product of two 1-body probabilities, strong correlation domains (SCD) of B are found. The emphasis is placed on the sensitivity of the condensates against B . No phase transitions in spin-structures are found. However, abrupt changes in the derivatives of observables (correlative probabilities) are found in some particular domains of B . In these domains the condensates are highly sensitive to B . The effect of temperature is considered. The probabilities defined in the paper can work as a bridge to relate theories and experiments. Therefore, they can be used to discriminate various spin-structures and refine the interactions.

PACS numbers: 03.75.Hh, 03.75.Mn, 75.10.Jm, 05.30.Jp

Submitted to: *J. Phys. A: Math. Gen.*

[‡] The corresponding author

1. Introduction

Bose-Einstein condensates are ideal artificial systems for quantum manipulation. The spinor condensates have very rich spin structures, and their swift response to the external field is notable [1]. Usually, a condensate would contain more than 10^4 atoms. Due to the progress in techniques, much smaller condensates (say, particle number $N \leq 1000$) could be produced. Note that the strength of the effective interaction between the particles C_2 is proportional to the average particle density, which is proportional to $N^{-3/5}$ (evaluated based on the Thomas-Fermi approximation). Thus the particles are subjected to a stronger interaction in smaller systems. In fact, in the study of spin-dynamics, the rate of evolution depends on $\tau = C_2 t / \hbar$ rather than t [2], where t is the time. Therefore, the evolution will be swifter in the smaller systems. Thus they might be even more suitable for manipulation. In principle, these systems could be more precisely prepared (such as N and M , the total magnetization, could be more rigorously given). Therefore, some properties not contained in large condensates might emerge (say, if $N < 50$, whether N is even or odd might be serious), and some properties might depend on the external field very sensitively in some particular cases (as shown below).

There are already a number of literatures dedicated to the large condensates of spin-1 atoms. The commonly used theoretical tool is the mean field theory (MFT) [3, 4, 5, 6, 7, 8, 9]. The ground states with the ferromagnetic phase and polar phase are found. Their modes of excitation and their dynamical behavior have been studied, and very rich physical phenomena have been found (say, the formation of spin-domains and spin-vortices). On the other hand, for small condensates, a theory goes beyond the MFT might be more appropriate. In this paper, the spin-structures of spin-1 small condensates under a magnetic field B are studied by using a many-body theory in which the parentage coefficients of spin-states are used as a tool [10, 11]. The variation of B is considered as adiabatic and the discussion is limited to static behavior. One-body and two-body spin correlative probabilities are defined and calculated. They are used to extract information from the spin eigenstates.[12] Furthermore, the correlation coefficients are defined and calculated to measure quantitatively the spin correlation, and the fidelity susceptibilities are also calculated to measure quantitatively the sensitivity of the ground states against the change of B . Thereby a detailed and deeper description on spin-spin correlation has been obtained that might lead to a better understanding on spin structures. In particular, the spin probabilities defined in this paper are observables, they might serve as a bridge to relate theories and experiments, therefore can be used to clarify various spin-structures and interactions. The emphasis is placed on the response of the condensates to B . The related knowledge might be useful for quantum manipulation. Both the cases with the temperature T zero and nonzero are considered.

2. Hamiltonian and the eigenstates

Let N spin-1 atoms be confined by an isotropic and parabolic trap with frequency ω . The interaction is $V_{ij} = \delta(\mathbf{r}_i - \mathbf{r}_j)(c_0 + c_2 \mathbf{f}_i \cdot \mathbf{f}_j)$, where \mathbf{r}_i and \mathbf{f}_i are, respectively, the position vector and the spin operator of the i -th particle. A magnetic field B lying along the Z -axis is applied. We consider the case that the size of the condensate is small so that it is smaller than the spin healing length. In this case, the single mode approximation (SMA) is applicable.[13] Under the SMA all particles will have the same spatial wave function $\phi(\mathbf{r})$. After the integration over the spatial degrees of freedom, we arrive at a model Hamiltonian

$$H_{\text{mod}} = C_2 \hat{S}^2 - p \sum_i \hat{f}_{iz} + q \sum_i (\hat{f}_{iz})^2, \quad (1)$$

where \hat{S} is the total spin operator of the N particles, $C_2 = c_2 \int d\mathbf{r} |\phi(\mathbf{r})|^4 / 2$, \hat{f}_{iz} is the z -component of \mathbf{f}_i , $p = -\mu_B B / 2$, $q = (\mu_B B)^2 / 4E_{\text{hf}}$, μ_B the Bohr magneton and E_{hf} the hyperfine splitting energy. The last two terms of H_{mod} are the linear and quadratic Zeeman energies, respectively.

The eigenstates of H_{mod} will have S and its z -component M (namely, the magnetization, $M \geq 0$ is assumed) conserved when the quadratic term is neglected. Therefore they can be denoted as ϑ_{SM}^N , $S = N, N - 2$, to 1 or 0. It has been proved that ϑ_{SM}^N is unique without further degeneracy [14]. They together form a complete set for all the totally symmetric spin-states of $f = 1$ systems. When the quadratic term is taken into account, M will remain to be conserved, but S will not. In this case ϑ_{SM}^N can be used as basis functions for the diagonalization of H_{mod} . In this approach, a powerful tool, the fractional parentage coefficients, that we have developed previously is used for the calculation of related matrix elements [10, 11].

Using these coefficients, a particle (say, the particle 1) can be extracted from ϑ_{SM}^N as

$$\vartheta_{SM}^N = \sum_{\mu} \chi_{\mu}(1) [a_{SM\mu}^{\{N\}} \vartheta_{S+1, M-\mu}^{N-1} + b_{SM\mu}^{\{N\}} \vartheta_{S-1, M-\mu}^{N-1}], \quad (2)$$

where $\chi_{\mu}(1)$ is the spin-state of the particle 1 in component $\mu = 0$ or ± 1 . The fractional parentage coefficients have analytical forms as

$$a_{SM\mu}^{\{N\}} = \sqrt{\frac{[1 + (-1)^{N-S}](N-S)(S+1)}{2N(2S+1)}} C_{1\mu, S+1, M-\mu}^{SM}, \quad (3)$$

$$b_{SM\mu}^{\{N\}} = \sqrt{\frac{[1 + (-1)^{N-S}]S(N+S+1)}{2N(2S+1)}} C_{1\mu, S-1, M-\mu}^{SM}, \quad (4)$$

where the Clebsch-Gordan coefficients are introduced.

Once a particle has been extracted, the calculation of the matrix elements is straight forward, and we have

$$\langle \vartheta_{S'M'}^N | H_{\text{mod}} | \vartheta_{SM}^N \rangle = \delta_{M', M} \{ \delta_{S'S} [C_2 S(S+1) - pM] + q Q_{S'S}^{NM} \}, \quad (5)$$

where

$$Q_{S'S}^{NM} \equiv N \langle \vartheta_{S'M}^N | (\hat{f}_{1z})^2 | \vartheta_{SM}^N \rangle = N \sum_{\mu} \mu^2 q_{S'S}^{NM\mu}, \quad (6)$$

$$q_{S'S}^{NM\mu} = \delta_{S'S} [(a_{SM\mu}^{\{N\}})^2 + (b_{SM\mu}^{\{N\}})^2] + \delta_{S',S-2} a_{S-2,M\mu}^{\{N\}} b_{SM\mu}^{\{N\}} \\ + \delta_{S',S+2} a_{SM\mu}^{\{N\}} b_{S+2,M\mu}^{\{N\}}. \quad (7)$$

For an arbitrary N , after a procedure of diagonalization, the set of eigenenergies E_i and the corresponding eigenstates $\Theta_{iM} = \sum_s d_S^{iM} \vartheta_{SM}^N$ can be obtained, where E_i is in the order of increasing energy. Since the set ϑ_{SM}^N is complete, the set Θ_{iM} is exact for H_{mod} .

3. Spin correlative probabilities

For the condensates with nonzero spins, it has been shown theoretically that there are various spin-structures. In order to confirm these structures experimentally, one has to define some measurable physical quantities. For the spatial degrees of freedom, it is reminded that the one-body density $\rho(\mathbf{r})$ can provide information on the spatial distribution of the particles, and the two-body density $\rho(\mathbf{r}_1, \mathbf{r}_2)$ can describe the spatial correlation. Similar quantities can be defined in the spin space. Each spin eigenstate can be written as

$$\Theta_{iM} = \sum_s d_S^{iM} \vartheta_{SM}^N = \sum_{\mu} \chi_{\mu}(1) \varphi_{\mu}^{iM}. \quad (8)$$

where φ_{μ}^{iM} can be obtained via Equation (2). The normality $1 = \langle \Theta_{iM} | \Theta_{iM} \rangle = \sum_{\mu} \langle \varphi_{\mu}^{iM} | \varphi_{\mu}^{iM} \rangle$ implies that $\langle \varphi_{\mu}^{iM} | \varphi_{\mu}^{iM} \rangle$ is the probability of particle 1 in μ -component. Then, we define the one-body probability

$$P_{\mu}^{i,M} \equiv \langle \varphi_{\mu}^{iM} | \varphi_{\mu}^{iM} \rangle = \sum_{SS'} d_{S'}^{iM} d_S^{iM} q_{S'S}^{NM\mu}. \quad (9)$$

Note that $NP_{\mu}^{i,M}$ is just the average population of the μ -component, and is an observable which can be directly measured via the Stern-Gerlach technique.

In the case with $B = 0$, S is a good quantum number, and the i -th state has $S_i = N + 2 - 2i$ (if $c_2 < 0$), or $S_i = 2(i - 1)$ (if $c_2 > 0$).[5] In this case, $d_S^{iM} = \delta_{S,S_i} d_{S_i}^{iM}$, and we have

$$P_{\mu}^{i,M} = (a_{S_i M \mu}^{\{N\}})^2 + (b_{S_i M \mu}^{\{N\}})^2. \quad (10)$$

When one more particle is extracted from the right side of Equation (2), we have

$$\vartheta_{SM}^N = \sum_{\mu,\nu} \chi_{\mu}(1) \chi_{\nu}(2) \sum_{S'} A_{\mu\nu,S'}^{NSM} \vartheta_{S',M-\mu-\nu}^{N-2}, \quad (11)$$

where

$$A_{\mu\nu,S+2}^{NSM} = a_{SM\mu}^{\{N\}} a_{S+1,M-\mu,\nu}^{\{N-1\}}, \quad (12)$$

$$A_{\mu\nu,S}^{NSM} = a_{SM\mu}^{\{N\}} b_{S+1,M-\mu,\nu}^{\{N-1\}} + b_{SM\mu}^{\{N\}} a_{S-1,M-\mu,\nu}^{\{N-1\}}, \quad (13)$$

$$A_{\mu\nu,S-2}^{NSM} = b_{SM\mu}^{\{N\}} b_{S-1,M-\mu,\nu}^{\{N-1\}}. \quad (14)$$

or $A_{\mu\nu,S'}^{NSM} = 0$ otherwise.

Then the i -th state can be rewritten as

$$\Theta_{iM} = \sum_{\mu,\nu} \chi_{\mu}(1)\chi_{\nu}(2)\varphi_{\mu\nu}^{iM}. \quad (15)$$

From the normality as before, we have $1 = \sum_{\mu,\nu} \langle \varphi_{\mu\nu}^{iM} | \varphi_{\mu\nu}^{iM} \rangle$. Thus, it is straight forward to define the 2-body spin correlative probability as

$$P_{\mu\nu}^{i,M} \equiv \langle \varphi_{\mu\nu}^{iM} | \varphi_{\mu\nu}^{iM} \rangle = \sum_{SS'S''} d_S^{iM} d_{S''}^{iM} A_{\mu\nu,S'}^{NSM} A_{\mu\nu,S'}^{NS''M}. \quad (16)$$

$P_{\mu\nu}^{iM}$ is the probability that the spin of a particle is in μ while another in ν when the two are observed, Obviously, $P_{\mu\nu}^{i,M} = P_{\nu\mu}^{i,M}$. If more particles are extracted, higher order spin correlative probabilities could also be similarly defined. These probabilities do not have a counterpart in the MFT, therefore additional information might be provided by them. Incidentally, the technique for the measurement of the correlative probabilities is mature in particle physics and nuclear physics, but not in condensed matter physics. The development of related technique is desired.

In general, one can define the correlation coefficient $\gamma_{\mu,\nu}^{i,M} \equiv P_{\mu\nu}^{i,M} / P_{\mu}^{i,M} P_{\nu}^{i,M}$ to measure quantitatively how large the correlation is. If $\gamma_{\mu,\nu}^{i,M}$ deviates remarkably from 1, the correlation is strong. Whereas if $\gamma_{\mu,\nu}^{i,M} \approx 1$, the correlation is weak, and the system can be well understood simply from the 1-body probabilities.

Numerical examples will be given below. $\hbar\omega$ and $\sqrt{\hbar}/(m\omega)$ are used as units for energy and length, respectively, where m is the mass of atom. The spatial wave function $\phi(\mathbf{r})$ is obtained under the Thomas-Fermi approximation, and thereby we have the strength $C_2 = 0.154c_2/(Nc_0)^{3/5}$. Since a slight inaccuracy that may exist in $\phi(\mathbf{r})$ would cause only a slight deviation in the magnitude of C_2 , the approximation is acceptable in the qualitative sense. $\omega = 300 \times 2\pi$ (in sec^{-1}) and $N = 1000$ are in general assumed (unless particularly specified). ^{87}Rb and ^{23}Na condensates will be used as examples for the $c_2 < 0$ and $c_2 > 0$ species, respectively. In the units adopted, we have $c_0 = 2.49 \times 10^{-3}\sqrt{\omega}$ and $c_2 = -1.16 \times 10^{-5}\sqrt{\omega}$ for ^{87}Rb , and $c_0 = 6.77 \times 10^{-4}\sqrt{\omega}$ and $c_2 = 2.12 \times 10^{-5}\sqrt{\omega}$ for ^{23}Na . The diagonalization of H_{mod} is straight forward when all the parameters are given. Then, the coefficients d_S^{iM} can be known. From Equations (9), (10) and (16), the 1-body and 2-body probabilities can be obtained.

4. Low temperature limit

The condensate will fall into its ground state Θ_{1M} with a specified M when $T = 0$. M is determined by how the species is prepared. The case with $T \neq 0$ will be considered later.

4.1. Condensates with $c_2 < 0$

To evaluate how strong the correlation in Θ_{1M} would be, the correlation coefficients $\gamma_{0,0}^{1,M}$ of Rb against B are shown in Figure 1(a). The magnitudes of all the curves are

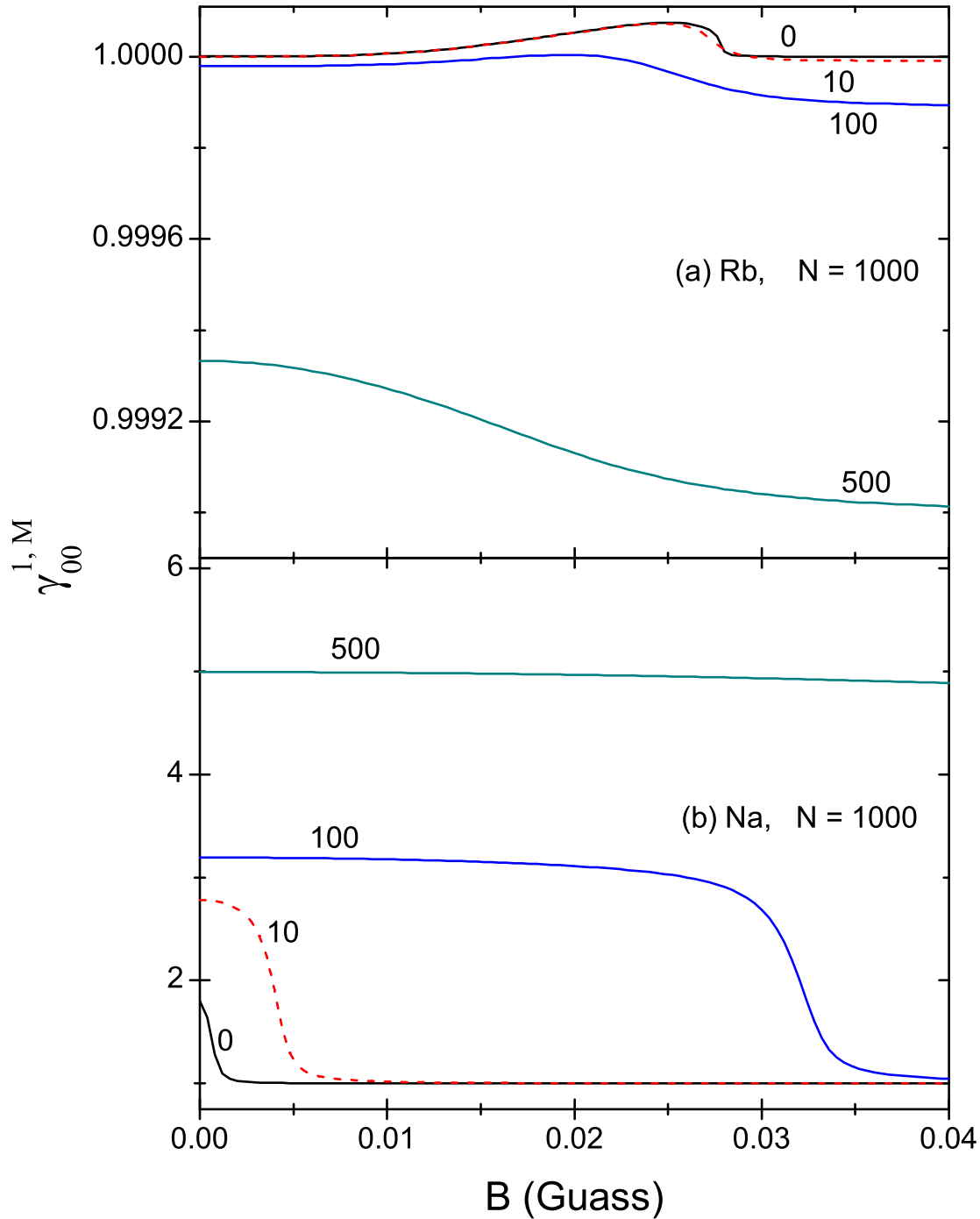


Figure 1. (Color online) The variation of the correlation coefficient $\gamma_{0,0}^{1,M}$ against B for the ground states of condensates with a specified M . $N = 1000$, $\omega = 300 \times 2\pi$ are assumed, and the experimental data for ^{87}Rb and ^{23}Na are adopted (also for the following figures, except particularly specified). M is given at four values marked beside the curves.

extremely close to one in (a). This is also true for $\gamma_{\mu,\nu}^{1,M}$ with $(\mu, \nu) \neq (0, 0)$. It implies that the correlation in Θ_{1M} is very weak.

When $B = 0$, Θ_{1M} will have $S = N$. [5, 15] Its expression does not depend on the

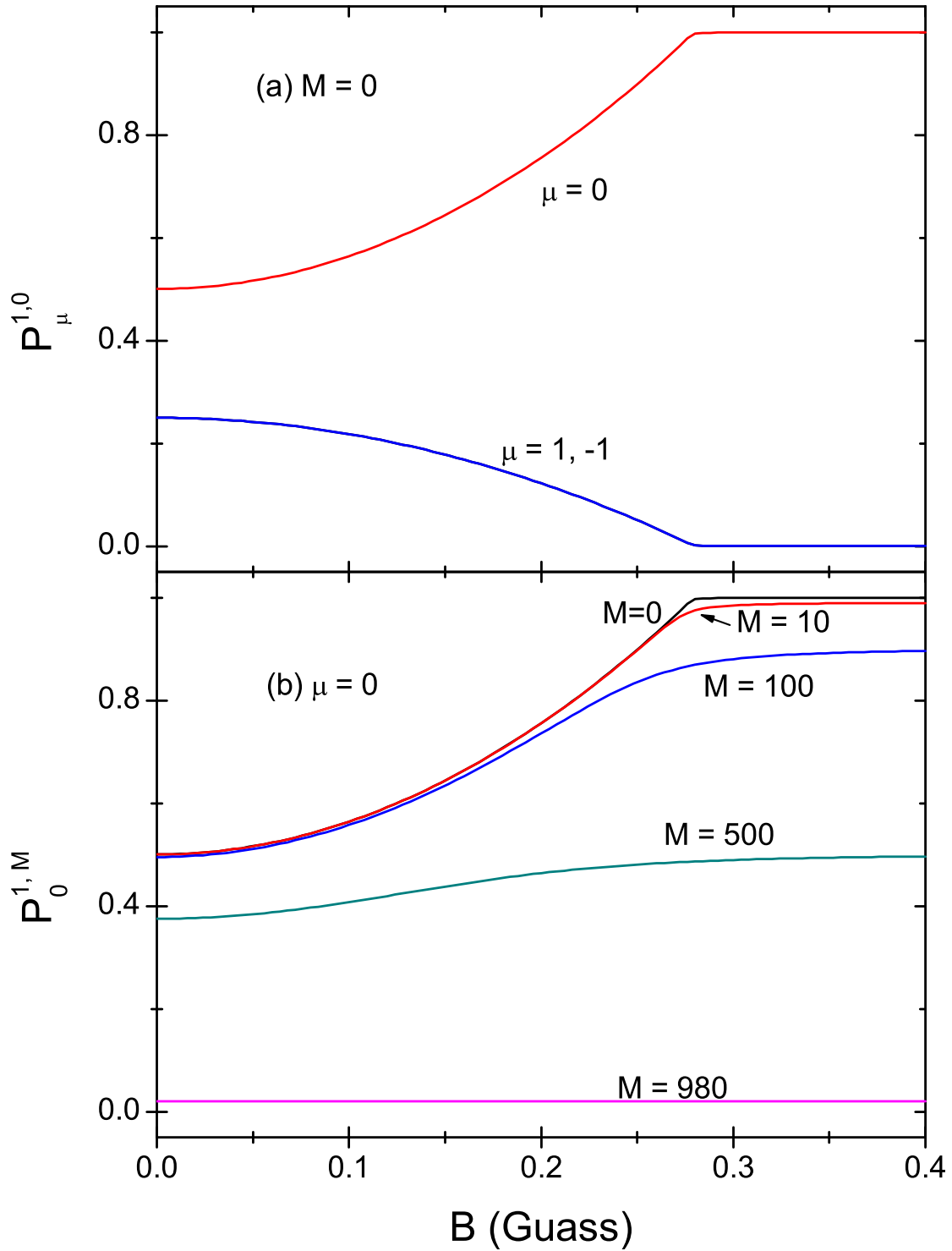


Figure 2. (Color online) $P_{\mu}^{1,M}$ of the ^{87}Rb condensate against B . (a) is for $M = 0$ and μ is marked beside the curves. (b) is for $\mu = 0$ and M is marked beside the curves.

details of interaction but only on the sign of c_2 , and can be uniquely written as

$$\Theta_{1,M} = \vartheta_{NM}^N \equiv (\cdots((\chi(1)\chi(2))_2\chi(3))_3 \cdots \chi(N))_{N,M}, \quad (17)$$

where $(\chi_A\chi_B)_\lambda$ implies that the spins of χ_A and χ_B are coupled to spin λ , and so on.

The special way of spin coupling in Equation (17) (i.e., the combined spin of an arbitrary group of j particles is j) assure that the state is normalized and symmetrized. Where all the spins are roughly aligned along a common direction, but the azimuthal angle of this direction is arbitrary.

From Equation (10) the analytical forms of $P_\mu^{1,M}$ can be derived as

$$P_{\pm 1}^{1,M} = \frac{(N \pm M)(N \pm M - 1)}{2N(2N - 1)}, \quad (18)$$

$$P_0^{1,M} = \frac{(N - M)(N + M)}{N(2N - 1)}. \quad (19)$$

Equation (19) can be approximately rewritten as $P_0^{1,M} \approx \frac{1}{2}(1 - \frac{M^2}{N^2})$. Thus, if $M = 0$, half of the particles would have $\mu = 0$. If $M \neq 0$, the increase of M would lead to a decrease of $P_0^{1,M}$. In particular, $P_0^{1,M} \rightarrow 0$ when $M \rightarrow N$ as expected. Incidentally, the above analytical forms of $P_\mu^{1,M}$ are identical to those from the MFT when $N \rightarrow \infty$. [6]

When B varies, the one-body probabilities $P_\mu^{1,M}$ of Θ_{1M} against B are calculated and shown in Figure 2. The left ends of the curves coincide exactly with those from the above analytical expressions. Note that the $\mu \neq 0$ particles will gain additional energy from the quadratic Zeeman term. In order to reduce the energy the number of $\mu = 0$ particles will increase with B . This is clearly shown in Figure 2. For $M = 0$ as shown in Figure 2a, the derivative of $P_0^{1,0}$ varies very swift from a positive value to zero at the vicinity of a turning point $B = 0.28G$ where $P_0^{1,0} \approx 1$, i.e, the number of $\mu = 0$ particles \bar{N}_0 is very close to its limit N . The swift variation at the turning point will become a sudden transition when N is large, and the point becomes a critical point B_{crit} . Passing through this point, the derivative varies abruptly, but the spin-state Θ_{10} itself varies continuously. When $B > B_{\text{crit}}$, the ground state remains unchanged as $\Theta_{10} = |0, N, 0\rangle \equiv (\chi_0)^N$, where $|N_1, N_0, N_{-1}\rangle$ is a Fock-state with N_1 , N_0 , and N_{-1} particles in $\mu = 1, 0$, and -1 , respectively.

When $M \neq 0$, not all the particles can be changed to $\mu = 0$ because of the conservation of M . Accordingly, the increase of $P_0^{1,M}$ is hindered and the curves in Figure 2b are smoother. When M is large, the curves are very flat implying that Θ_{1M} is affected by B very weakly. When $B \rightarrow \infty$, we found that $\Theta_{1,M} \rightarrow |M, N - M, 0\rangle$. Accordingly, $P_0^{1,M} \rightarrow (N - M)/N$, $P_1^{1,M} \rightarrow M/N$, and $P_{-1}^{1,M} \rightarrow 0$. In this way, $N_0 = N - M$ is maximized so that the quadratic Zeeman energy is minimized.

In conclusion of this section for small condensates of Rb, the ground state $\Theta_{1,M}$ is continuously changed from ϑ_{NM}^N to $|M, N - M, 0\rangle$ without a transition when B increases. However, the derivative $\frac{d\bar{N}_0}{dB}$ undergoes a transition at B_{crit} when $M = 0$. It is recalled that the MFT, which is correct when N is very large, has predicted the transitions between the ferromagnetic, broken-axisymmetry, and the polar phases [3, 8, 9]. The broken-axisymmetry phase is caused by a rapid quenched field, therefore it is not expected to appear in our case with B varying adiabatically..

4.2. Condensates with $c_2 > 0$

Contrary to the previous case, the spin correlation is very strong in the ground states $\Theta_{1,M}$ of $c_2 > 0$ condensates as shown by $\gamma_{0,0}^{1,M}$ in Figure 1b, where the left ends of all the curves are remarkably larger than 1. It implies that, when two particles are observed, the probability of a particle in $\mu = 0$ would be much larger if the other one has $\nu = 0$. Starting from $B = 0$ there is a domain of B where $\gamma_{0,0}^{1,M}$ remains large and nearly unchanged (refer to the $M = 100$ curve in Figure 1b). Outside the domain, the correlation vanish rapidly. The domain is called a strong correlation domain (SCD), where the spin-structure at $B = 0$ will keep unchanged against the increase of B . The SCD does not have a clear border. For each curve in Figure 1b, let B_{scd} be the value where $\gamma_{0,0}^{1,M} = [(\gamma_{0,0}^{1,M})_{\text{max}} + 1]/2$. Then, B_{scd} is considered as the outward border of the SCD. A larger M will lead to a larger B_{scd} (say, for Figure 1b, if $M = 10, 100,$ and $500,$ respectively, $B_{\text{scd}} \approx 0.0041G, 0.0318G,$ and $0.153G$). Thus the spin structure at $B = 0$ will better keep when M is large.

When $B = 0$, the ground state will have S as small as possible.[5, 15] Thus, $\Theta_{1,M} = \vartheta_{M,M}^N$ if $N - M$ is even, or $= \vartheta_{M+1,M}^N$ if $N - M$ is odd. Due to the fact that $\vartheta_{S,M}^N$ is unique, we have

$$\vartheta_{M,M}^N \propto \mathcal{P}\{(\chi_1)^M [(\chi\chi)_0]^{(N-M)/2}\}, \quad (20)$$

where \mathcal{P} is the symmetrizer, i.e., a summation over the $N!$ particle permutations. So this state is composed of a group of $\mu = 1$ particles together with a group of singlet pairs. And

$$\vartheta_{M+1,M}^N \propto \mathcal{P}\{\vartheta_{M+1,M}^{M+1} [(\chi\chi)_0]^{(N-M-1)/2}\}, \quad (21)$$

which is composed of a group of $M + 1$ polarized particles (but the direction of polarization deviates a little from the Z-axis) together with a group of singlet pairs. From Equation (10) the one-body probabilities are

$$P_0^{1,M} = \frac{|M|(2 + 1/N) - 2|M|^2/N - 1}{(2|M| + 3)(2|M| - 1)}, \quad (22)$$

$$P_{\pm 1}^{1,M} = \frac{|M|(2 - 1/N) + |M|^2(4 + 2/N) \pm M(4|M|(|M| + 1) - 3)/N - 2}{2(2|M| + 3)(2|M| - 1)} \quad (23)$$

For the case $M = 0$ and N being even, $\Theta_{1,M} = \vartheta_{0,0}^N \propto \mathcal{P}([(\chi\chi)_0]^{N/2})$. This state is named the polar state where all the particles are in the singlet pairs. From Equations. (22) and (23), the polar state has $P_\mu^{1,0} = 1/3$ for all μ . In other words, the particles are equally populated among the three components. This is a common property of $S = 0$ states.

When B increases, $P_\mu^{1,M}$ against B are shown in Figure 3. Since the ground state will have more and more $\mu = 0$ particles, $P_0^{1,0}$ increases sharply from $1/3$ to ≈ 1 as shown in Figure 3a. Correspondingly, the ground state $\Theta_{1,0}$ is sharply transformed from $\vartheta_{0,0}^N$ to $|0, N, 0\rangle \equiv (\chi_0)^N$. Comparing the curve of $P_0^{1,0}$ in Figure 3a with the one in Figure 2a for Rb, the rise of the former is much faster than the latter. Thus the Na condensate is highly sensitive to the appearance of B if $M = 0$. A very weak field (a

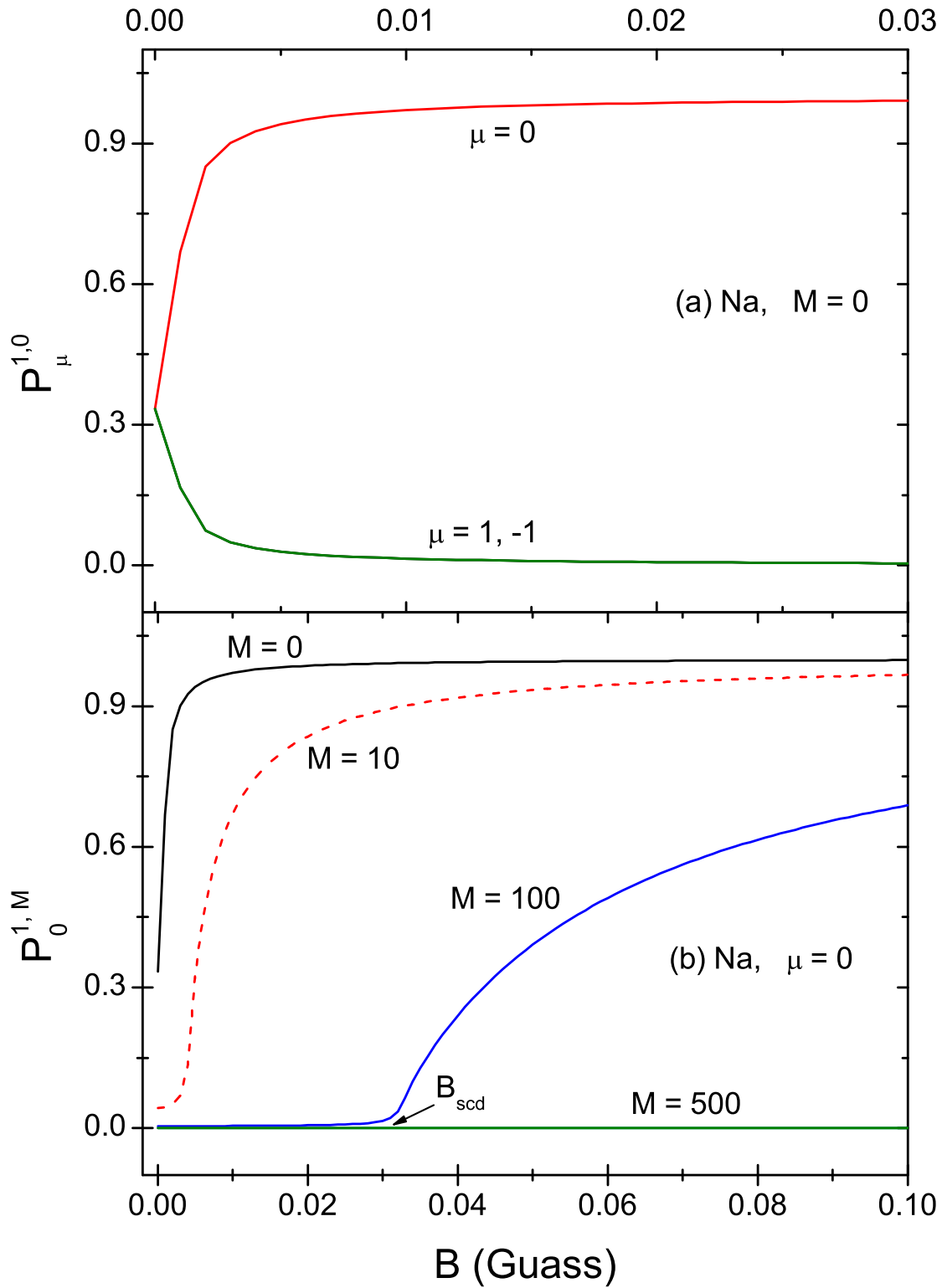


Figure 3. (Color online) The same as Figure 2 but for the ^{23}Na condensates.

few mG) is sufficient to break nearly all the pairs and turn every spin lying on the X - Y plane independently. The independence is supported by the curve of $\gamma_{0,0}^{1,0}$ in Figure 1b,

where $\gamma_{0,0}^{1,0} \approx 1$ except B is close to zero. However, the high sensitivity will be lost when $M \neq 0$.

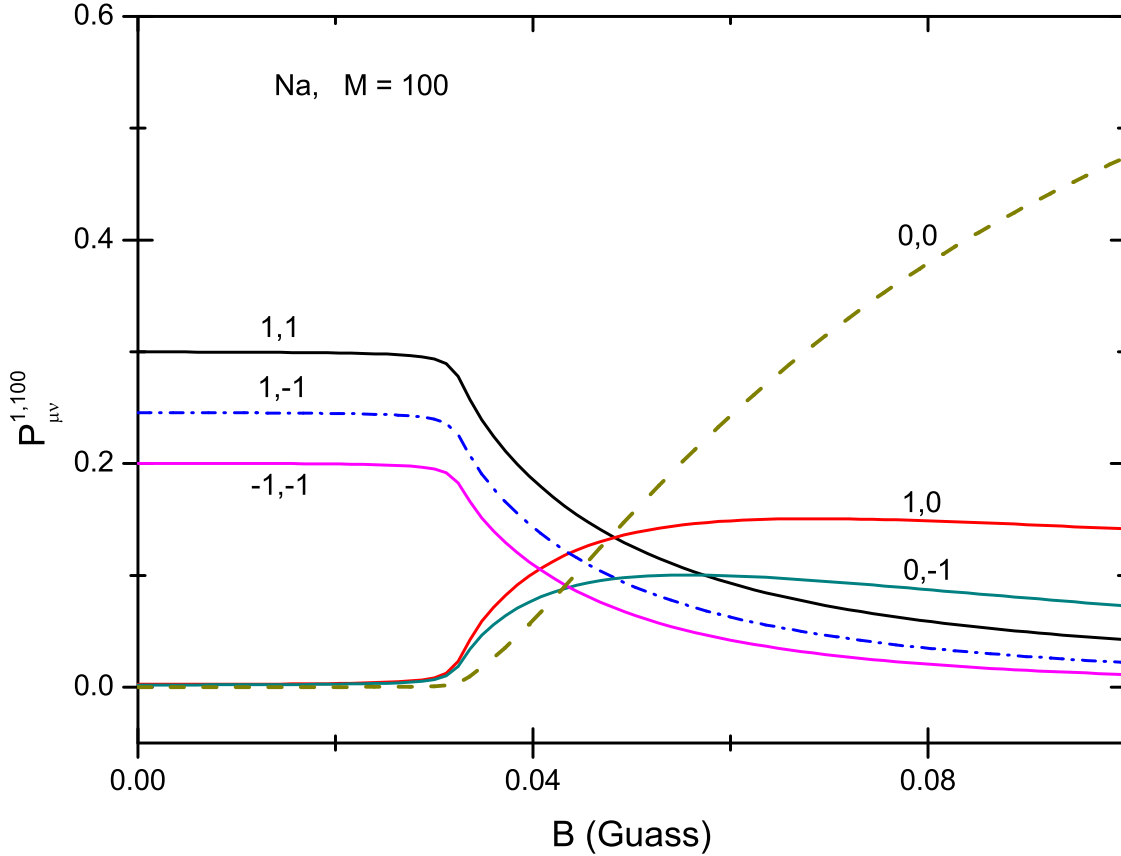


Figure 4. (Color online) Correlative probabilities $P_{\mu\nu}^{1,100}$ of the ^{23}Na condensate against B . (μ, ν) is marked beside the curves.

In Figure 3b the curve of $P_0^{1,100}$ remains to be horizontal when $B < B_{\text{scd}} = 0.0318G$ (refer also to the curve with $M = 100$ in Figure 1b). Thus the spin-structure inside the SCD might remain unchanged. To clarify, the 2-body probabilities are calculated and shown in Figure 4, where all the $P_{\mu\nu}^{1,M}$ remain unchanged in the SCD. Thus the invariance of the structure against B is strongly supported. The invariance can also be seen by observing the overlap $\langle \Theta_{1,M}^{B=0} | \Theta_{1,M}^B \rangle^2 = \langle \vartheta_{M,M}^N | \Theta_{1,M}^B \rangle^2 = (d_M^{1,M})^2$ against B (N and M are assumed to be even, a superscript B is added to emphasize the dependence on B). With the parameters of Figure 3 and with $M = 100$, this overlap is ≥ 0.99 when $B \leq 0.02G$. Thus the invariance is directly confirmed. However, it decreases very fast when B is close to B_{scd} , and is equal to 0.58 when $B = B_{\text{scd}}$. Afterward, it tends to zero rapidly when B is further larger. The existence of the SCD demonstrates that the mixture of a group of singlet pairs together with a group of M unpaired particles (each has $\mu = 1$) is capable to keep its structure against B . However, the capability will be lost when B is close to or $> B_{\text{scd}}$. Afterward the mixture will begin to change. Note that the change is characterized by the increasing of $\mu = 0$ particles, which come from the breaking of pairs. Therefore the change would be less probable if the original

number of pairs is small. Thus a larger M (implying a fewer original pairs) will lead to a better stability and therefore a larger B_{scd} . A larger c_2 will also lead to a better stability and therefore a larger B_{scd} (say, if c_2 is one time larger than the experimental value of $(c_2)_{\text{Na}}$, then the B_{scd} would be enlarged from $0.0318G$ to $0.0465G$ for the curve with $M = 100$ in Figure 3b).

Since M affects the stability, $P_\mu^{1,M}$ is in general sensitive to M . If B is weak, the sensitivity would be very high when M is small. E.g., it is shown in Figure 3b that $P_0^{1,M}$ will decrease dramatically at $B = 5mG$ when M/N is simply changed from 0 to 0.01.

When $B \rightarrow \infty$, all the pairs will be destroyed and $\Theta_{1,M}$ will tend to $|M, N - M, 0\rangle$. Thus, disregarding $c_2 < \text{or} > 0$, both species tend to the same structure.

4.3. Fidelity susceptibility

In order to understand the sensitivity of the ground states $\Theta_{1,M}^B$ against B quantitatively, the fidelity susceptibility [16, 17, 18].

$$\Gamma_M(B) = \lim_{\varepsilon \rightarrow 0} \frac{2}{\varepsilon^2} (1 - |\langle \Theta_{1,M}^{B+\varepsilon} | \Theta_{1,M}^B \rangle|), \quad (24)$$

is calculated and given in Figure 5. This figure demonstrates that each species has its own region highly sensitive to B . For Rb, the most sensitive region is surrounding the critical point B_{crit} where the increase of \bar{N}_0 stops suddenly (refer to Figure 2a). When B is small, the sensitivity does not depend on M and is in general very weak. Whereas for Na, the most sensitive region is surrounding the border of SCD, B_{scd} , where \bar{N}_0 begin to increase suddenly (refer to Figure 3b). The fact that B_{scd} will become larger with M is clearly shown in Figure 5b. The sensitivity can be very high when B is small if M is also small.

4.4. Effect of the trap and the particle number

Since the linear Zeeman term does not affect the spin-structures, the ratio q/C_2 involved in H_{mod} is crucial. This quantity is proportional to $B^2/\omega^{6/5}$. Therefore, a larger ω would reduce the effect of B . Consequently, for $\omega' > \omega$, all the curves plotted in Figure 1 to Figure 4 will extend horizontally to the right by a common factor $(\omega'/\omega)^{3/5}$. In particular, the SCD will become larger (say, B_{scd} of the ground states $\Theta_{1,100}$ of Na would increase from $0.0318G$ to $0.0655G$ if ω is from $300 \times 2\pi$ to $1000 \times 2\pi$).

On the other hand, the change of N causes not simply a change of scale, because the numbers of degrees of freedom are thereby changed. For an example, if $N = 1000, 100$, and 10 , $P_0^{1,0}$ of Rb would be $= 0.99$ when $B = 0.277G, 0.178G$, and $0.134G$, respectively. Thus, the curve of $P_0^{1,0}$ in Figure 2a would rise up faster if N decreases from 1000. On the contrary, if $N = 1000, 100$, and 10 , $P_0^{1,0}$ of Na would be $= 0.90$ when $B = 0.003G, 0.018G$, and $0.070G$, respectively. Thus, the curve of $P_0^{1,0}$ in Figure 3a would rise up slower if N decreases from 1000. Thus, the effect of N on $c_2 < 0$ and > 0 species is different.

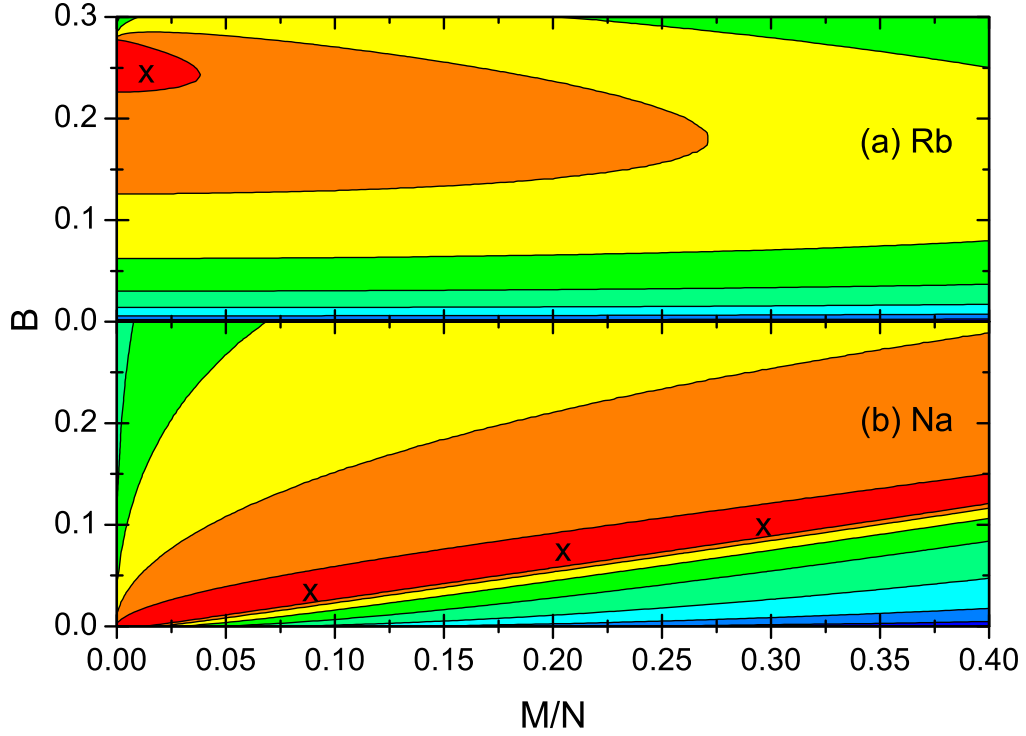


Figure 5. (Color online) $\ln(\Gamma_M(B))$ against M/N and B for the ground states of Rb (a) and Na (b) condensates. B is in Gauss and $N = 1000$. The maximum of $\ln(\Gamma_M(B)) = 10.65$ (a) or 11.20 (b). The region surrounding the maximum is marked with "X". The innermost contour of the X-region has the value 9.275 (a) or 9.078 (b). The difference of the values of a contour and its adjacent outer contour is 1.375 (a) or 2.122 (b).

The effect of N on $P_0^{1,M}$ with $M \neq 0$ is shown in Figure 6. The curve with $N = 1000$ in Figure 6a is identical to the curve with $M = 100$ in Figure 2b for $c_2 < 0$. In Figure 6a for Rb the curves with a smaller N will rise up faster against B just as the previous case with $M = 0$. For $c_2 > 0$, the curve with $N = 1000$ in Figure 6b is identical to the curve with $M = 100$ in Figure 3b. Similar to the case with $M = 0$, a smaller N will cause also a smoother change. In particular, the abrupt change appearing in the vicinity of B_{scd} as shown in Figure 3b will disappear when N is small.

5. Finite temperature

Since the level density in a condensate is usually dense, thermo-fluctuation is in general not negligible. What actually measured is the weighted probabilities $\bar{P}_\mu^M \equiv \sum_i W_i P_\mu^{i,M}$ and $\bar{P}_{\mu\nu}^M \equiv \sum_i W_i P_{\mu\nu}^{i,M}$, where $W_i = \exp(-E_i/k_B T) / \sum_j \exp(-E_j/k_B T)$ is the weight, E_i the energy, T the temperature, and the summation in principle runs over all the states. However, when $T \ll \hbar\omega/k_B \equiv T_0$, the contribution arises essentially from the ground band, and all the higher states can be neglected.[15] The members of the ground band have nearly the same spatial wave functions, and their spin-states together with E_i can

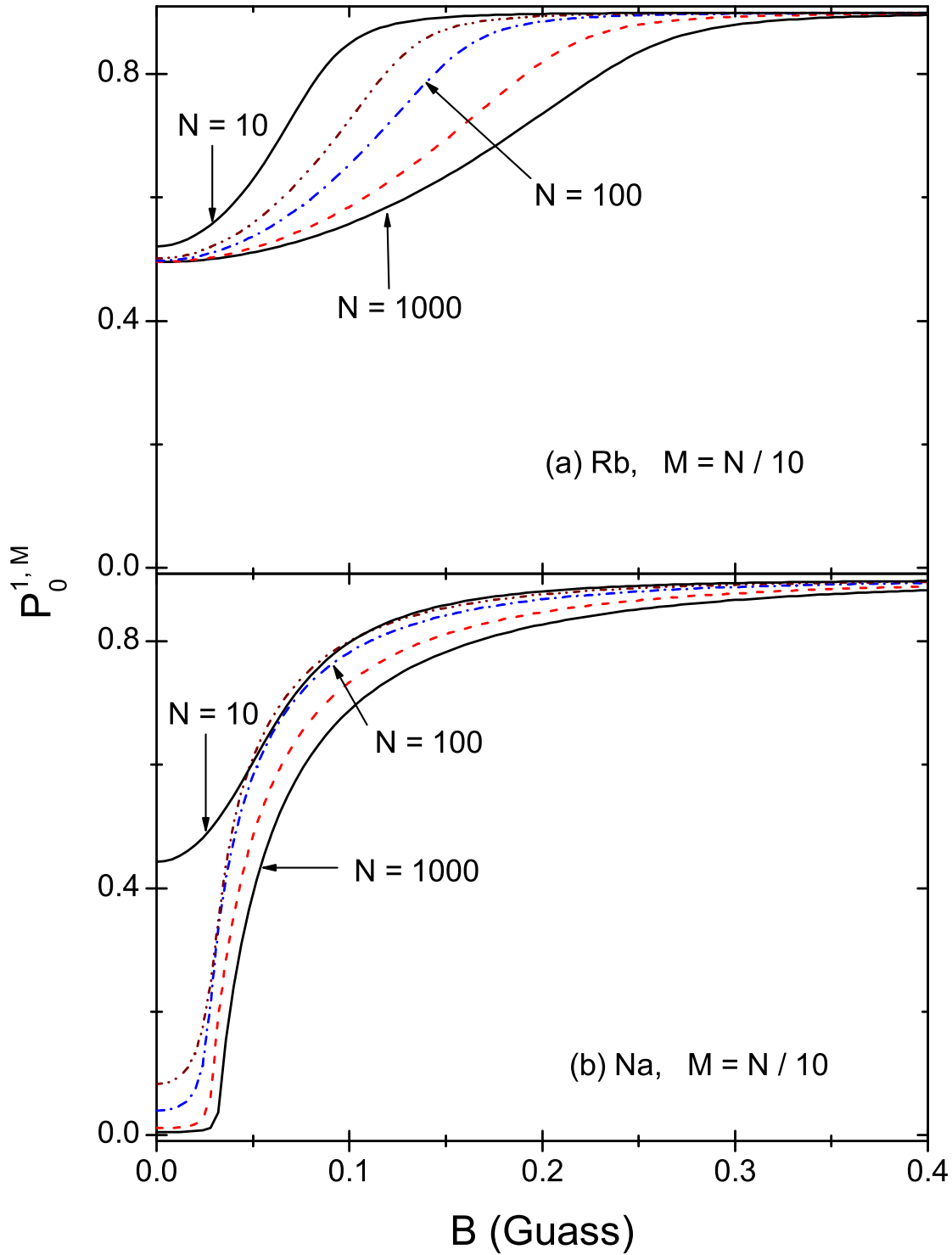


Figure 6. (Color online) $P_0^{1,M}$ against B with $M = N/10$ and N is given at five values: $N = 1000$ (solid line), 400 (dash), 100 (dash-dot), 40 (dash-dot-dot) and 10 (solid).

be obtained via the diagonalization of H_{mod} .

As an example, $\bar{P}_0^{(0)}$ of the condensates with $c_2 < 0$ at $T = T_0/10$ is plotted in Figure 7a. In order to see the effect of interaction, c_2 is given at three values. When B

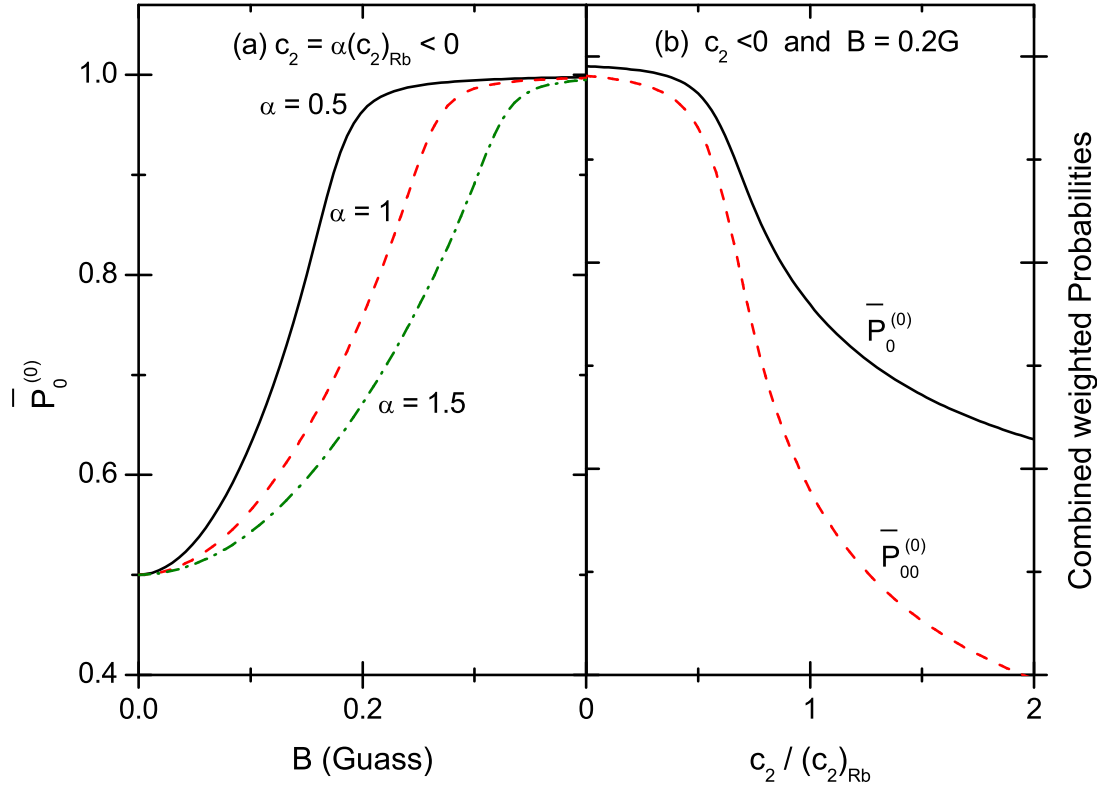


Figure 7. (Color online) The weighted probabilities for the condensates with $c_2 < 0$. $T = T_0/10$ is assumed and $c_0 = (c_0)_{\text{Rb}}$ (i.e., the experimental value of ^{87}Rb) and $c_2 = \alpha(c_2)_{\text{Rb}}$ are adopted. (a) $\bar{P}_0^{(0)}$ against B with α given at three values marked beside the curves. The dash curve has $\alpha = 1$. (b) $\bar{P}_0^{(0)}$ and $\bar{P}_{00}^{(0)}$ against α with $B = 0.2G$.

is very small ($< 0.02G$) or sufficiently large ($> 0.35G$), the three curves associated with different values of c_2 overlap nearly. However, in between, they are rather sensitive to c as shown in Figure 7a.. To see clearer, both $\bar{P}_0^{(0)}$ and $\bar{P}_{00}^{(0)}$ against c_2 under $B = 0.2G$ are plotted in Figure 7b. The figure demonstrates that the weighted 2-body probabilities are very sensitive to c_2 . Furthermore, the patterns of the curves can be tuned by altering B . Therefore, the measurement of the weighted probabilities under various B can provide rich information on the parameters of interaction.

One more example for the case $c_2 > 0$ is shown in Figure 8. Similar to the previous case, high sensitivity to the interaction is found. In Figure 8a, the left ends of the curves are flat. This is caused by the existence of the SCD, where the spin-structure remains nearly unchanged.

6. Final remarks

We have studied the spin structures of small spin-1 condensates ($N \leq 1000$) under a magnetic field B . The theory is beyond the MFT, and the single mode approximation has been adopted. The fractional parentage coefficients have been used as a tool for the

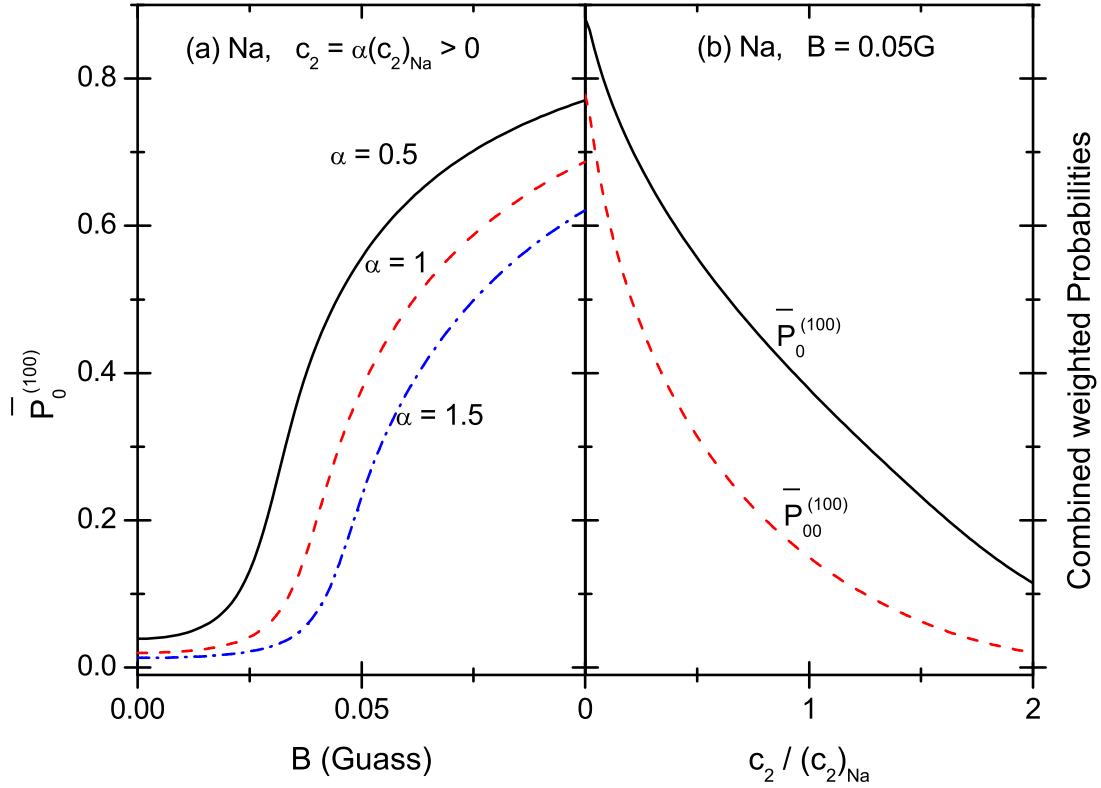


Figure 8. (Color online) Similar to Figure 7 but for the condensates with $c_2 > 0$ and $M = 100$. $c_0 = (c_0)_{\text{Na}}$ and $c_2 = \alpha(c_2)_{\text{Na}}$ are adopted. Refer to Figure 7.

analytical derivation. The 1-body, 2-body, and weighted probabilities are defined and calculated to extract information from the spin eigenstates. The correlation coefficients $\gamma_{\mu\nu}^{i,M}$ and the fidelity susceptibility $\Gamma_M(B)$ have also been calculated. The following results are mentioned ($N - M$ is assumed to be even for simplicity).

(i) When $B = 0$, the ground state $\Theta_{1,M}$ is either the ferromagnetic state ϑ_{NM}^N if $c_2 < 0$, or is the polar state $\vartheta_{M,M}^N$ if $c_2 > 0$. For ϑ_{NM}^N , all the N spins are coupled to total spin $S = N$, $\gamma_{\mu\nu}^{1,M}$ is close to 1 and $\Gamma_M(0)$ is very small (Figure 1 and Figure 5), therefore the ferromagnetic state does not have spin-correlation, and is inert to B when B is small. The state $\vartheta_{M,M}^N$ has M particles in χ_1 together with $(N - M)/2$ singlet pairs, its $\gamma_{0,0}^{1,M}$ is very large. Thus the polar state contains strong spin-correlation. Furthermore, its $\Gamma_M(B = 0)$ is very large when M is small. It implies a high sensitivity against the appearance of B .

(ii) When B increases, the number of $\mu = 0$ particles \bar{N}_0 in $\Theta_{1,M}$ will in general increase so as to reduce the quadratic Zeeman energy. For $c_2 < 0$, $\Theta_{1,M}$ will be changed from ϑ_{NM}^N to $|M, N - M, 0\rangle$ when B is from 0 to ∞ . The change goes on continuously, no transition in spin-structure occur. In accord with the change of $\Theta_{1,M}$, \bar{N}_0 is changed from $\frac{(N-M)(N+M)}{(2N-1)} \approx \frac{(1+M/N)}{2}(N - M)$ (refer to Equation (19)) to $N - M$. Therefore, $(\bar{N}_0)_{B \rightarrow \infty} - (\bar{N}_0)_{B=0} \approx (N - M)^2 / 2N \equiv N_{0,diff}$, which is the maximal number of particles allowed to be changed from being $\mu \neq 0$ to $\mu = 0$. When M is close to N , $N_{0,diff}$ is

very small implying that the room left for changing is very small, therefore $\Theta_{1,M}$ is inert to B (refer to Figure 2b where the curve with $M = 980$ is very flat). When M is smaller, $\Theta_{1,M}$ has much room for changing and therefore would be more sensitive to B . In particular, when $M = 0$, there is a critical point B_{crit} . Once $B \geq B_{\text{crit}}$ $(\bar{N}_0)_B = N$ and the ground state varies with B no more. There is an abrupt change in the derivative $\frac{d\bar{N}_0}{dB}$ at B_{crit} . Thus, although the spin-structures vary continuously with B , the related derivatives might not. B_{crit} is equal to $0.28G$ in Figure 2. It will be smaller when N decreases, and larger when ω increases.

(iii) For $c_2 > 0$, the increase of B from 0 to ∞ causes a change of $\Theta_{1,M}$ from ϑ_{MM}^N (or $\vartheta_{M+1,M}^N$) to $|M, N - M, 0\rangle$. $\Theta_{1,M}$ of both cases $c_2 < 0$ and > 0 tend to the same state because it is the most advantageous state for reducing the quadratic Zeeman energy. The change of $\Theta_{1,M}$ goes on also continuously without transitions. In this process \bar{N}_0 is in general increasing via a mechanism, i.e., a breaking of pairs as $(\chi\chi)_0 \rightarrow \chi_0\chi_0$ (whereas the process $(\chi\chi)_0 \rightarrow \chi_1\chi_{-1}$ is suppressed under B because it causes an increase of quadratic Zeeman energy). It is recalled that the particle correlation in $\Theta_{1,M}$ is very weak when $c_2 < 0$, but strong when $c_2 > 0$ due to the formation of pairs. When all the particles are paired (i.e., $M = 0$), the structure is extremely sensitive to B . A very weak B (a few mG) is sufficient to break all the pairs. For a comparison, $P_0^{1,0}$ in Figure 2a for Rb will be equal to 0.9 when $B = 0.25G$, but only = 0.003 G in Figure 3a for Na. However, when unpaired particles emerge (i.e., $M \neq 0$), the pairs will have an additional ability to keep themselves. The mechanism underlying this phenomenon deserves to be studied further. This leads to the appearance of SCD ranging from $B = 0$ to B_{scd} . A larger M will lead to a larger B_{scd} , while $B_{\text{scd}} = 0$ when $M = 0$. The spin-structure will remain unchanged when $B < B_{\text{scd}}$, but \bar{N}_0 will begin to increase when $B > B_{\text{scd}}$. The derivative of the probabilities varies very swiftly in the vicinity of B_{scd} . The swift variation will become a sudden jump when N is large (refer to Figure 6b). Thus B_{scd} is also a critical point when N is large. As a numerical example, when $N = 1000$ and $M = 100$, $B_{\text{scd}} = 0.03G$ in Figure 3b. Similar to B_{crit} , B_{scd} will become smaller when N decreases (with M/N remaining unchanged), and will become larger when ω increases.

(iv) The sensitivity of the ground states against B is quantitatively shown in Figure 5.

(v) When B is appropriately chosen and T is sufficiently low, the measurable weighted probabilities may provide rich information on the parameters of interaction.

Acknowledgments

The suggestion on the calculation of the fidelity and the comment from Prof. D. X. Yao is gratefully appreciated. The support from the NSFC under the grant 10874249 is also appreciated.

References

- [1] Sadler L E, Higbie J M, Leslie S R, Vengalattore M, and Stamper-Kurn D M 2006 *Nature* (London) **443** 312.
- [2] Luo M, Bao C G, and Li Z B 2008 *Phys. Rev. A* **77** 043625.
- [3] Stenger J, Inouye S, Stamper-Kurn D M, Miesner H J, Chikkatur A P and Ketterle W 1998 *Nature* (London) **396** 345.
- [4] Ho T L 1998 *Phys. Rev. Lett.* **81** 742.
- [5] Law C K, Pu H, and Bigelow N P 1998 *Phys. Rev. Lett.* **81** 5257.
- [6] Zhang W Z, Zhou D L, Chang M S, Chapman M S, and You L 2005 *Phys. Rev. A* **72** 013602.
- [7] Yi S, and Pu H 2006 *Phys. Rev. A* **73** 023602.
- [8] Isoshima T and Yip S 2006 *arXiv:cond-mat/0607630*.
- [9] Murata K, Saito H, and Ueda M 2007 *Phys. Rev. A* **75** 013607.
- [10] Bao C G 2004 *Acta Scientiarum Naturalium Universitatis Sunyatseni* **43** 70.
- [11] Bao C G and Li Z B 2005 *Phys. Rev. A* **72** 043614.
- [12] He Y Z and Bao C G 2011 *Phys. Rev. A* **83** 033622.
- [13] Chang M S, Qin Q, Zhang W X, You L, and Chapman M S 2005 *Nature Physics* **1** 111.
- [14] Katriel J 2001 *J. Mol. Struct.: THEOCHEM* **547** 1.
- [15] Bao C G and Li Z B 2004 *Phys. Rev. A* **70** 043620.
- [16] You W L, Li Y W, and Gu S J 2007 *Phys. Rev. E* **76** 022101.
- [17] Quan H T, Song Z, Liu X F, Zanardi P, and Sun C P 2006 *Phys. Rev. Lett.* **96** 140604.
- [18] Zanardi P, Giorda P, and Cozzini M 2007 *Phys. Rev. Lett.* **99** 100603.